J. Condensed Matter Nucl. Sci. 10 (2013) 46–62

Research Article

Effect of Forced Oxidation on Hydrogen Isotope Absorption/Adsorption Characteristics of Pd–Ni–Zr Oxide Compounds *

Yuki Miyoshi, Hideyuki Sakoh, Akira Taniike, Akira Kitamura † ‡

Graduate School of Maritime Sciences, Kobe University, 5-1-1 Fukaeminani-machi, Higashinada-ku, Kobe 658-0022, Japan

Akito Takahashi §, Reiko Seto and Yushi Fujita

Technova Inc., Uchisaiwaicho 1-1-1, Chiyodaku, Tokyo 100-0011, Japan

Abstract

Deuterium and protium gas absorption/adsorption by 0.1-μmϕ Pd powder (PP), Pd-black (PB), Pd nano-particles ($\sim$10 nmϕ) admixed with ZrO_2 (PZ) and Pd·Ni binary nano-particles ($\sim$2 nmϕ) dispersed in ZrO_2 holder-flakes (PNZ2B) has been examined. For the PP, the PB and the PZ samples, both the deoxidized samples and those reused without baking process showed essentially the same values of the loading ratio D(H)/Pd, the specific output energy E_1 and the hydridation energy $Q_{D(H)}$ which are consistent with the published values for bulky samples. For the as-received and oxidized samples both D(H)/Pd and E_1 are increasing functions of fineness of the Pd surface, and exceeds 2.0 and 1.5 eV/atom-Pd, respectively, for the PZ sample, giving the hydridation energy larger than the published value of the surface adsorption energy of 0.5 eV for bulky Pd samples. A rather large isotope effect in the differential heat of sorption, $\eta_{D(H)}$, has sometimes been observed in the 1a-phase characteristic of the oxygen-treated samples. The $Pd_{0.04}Ni_{0.29}Zr_{0.67}$ oxide composite sample, PNZ2B, has unique properties: Both D(H)/[Pd·Ni] $\approx$ 3.0 and E_1 $\approx$ 1.4 eV/atom-[Pd·Ni] for the as-received, the oxidized and deoxidized sample runs are very large, while $Q_{D(H)}$ = 0.50$\pm$ 0.1 eV/atom-D(H) for all cases is modest. It is inferred that the Pd atoms act as a catalyst for the hydrogen isotope absorption/adsorption of Ni at room temperature. From the fact that the No. 2 run after the forced deoxidation has essentially the same values of the absorption parameters as those of the No. 1 and No. 3 runs, it is inferred that the surface adsorption potential is made shallower in the PNZ2B sample than in Pd-based samples. The ratio η_D/η_H is sometimes greater than 1.5, which appears to be suggesting the existence of heat component of nuclear origin.
 ISSN 2227-3123

Keywords: Anomalous heat, Deuterium absorption, Differential heat of hydrogen uptake, Forced oxidation, Isotope effect,

© 2013 ISCMNS. All rights reserved. ISSN 2227-3123

Loading ratio, Pd·Ni·Zr nano-composite

1. Introduction

Palladium has been one of the most interesting and important elements for catalysis, hydrogen storage and purification for many years, and extensive works have been done. Among them, the most important researches are those on the isotope effect of absorption by 10-μm-thick Pd film [1] and on the particle size effect on the absorption characteristics [2,3].

Palladium has also been the key element for condensed matter nuclear phenomena, the so-called cold fusion [4]. Arata and Zhang [5] reported that highly pure D_2 gas charging of Pd nano-powders in the form of Pd/ZrO_2 induced significantly higher temperatures inside the reactor vessel than at the outside wall continuing for more than 50 h, while runs with H_2 gas showed almost no temperature difference. To verify that the excess heat originated in a nuclear process, a quadrupole mass spectrometer was employed to show the existence of significant amount of ^{4}He as nuclear ash in the vessel and in the powder after the charging. The charging system is a sophisticated, yet simplified, version of the previous-generation DS reactor [6].

Since then, the gas-phase charging systems have been another important method to induce possible anomaly in heat generation. Successful replications using systems similar to the DS reactor with Pd-black have been reported by Kirkinski et al. [7], Biberian et al. [8] and Celani et al. [9]. On the other hand, Kidwell et al. [10], Hioki et al. [11,12], and Dmitriyeva et al. [13] have also developed independently gas absorption systems with precise calorimetry equipments for samples of Pd-loaded zeolites and/or alumina.

A more sophisticated system has been developed also in our laboratory [14–18]. Our system is a twin absorption system, which enables simultaneous mass-flow-calorimetry for D_2 and H_2 gas absorption. We have used commercially available powder samples and those supplied by Santoku Corporation.

On the other hand, B. Ahern (BA), Vibronic Energy Technologies Corporation, fabricated his own samples of Pd·Ni·Zr oxide compounds by melt-spinning method to perform gas absorption and temperature measurement. He reported very large loading ratio of hydrogen and heat evolution [19]. He offered us the sample to perform precise calorimetry in our twin-absorption system. The present paper describes the comprehensive results of time-dependent measurements of hydrogen isotope gas absorption/adsorption (sorption) at room temperature and associated heat evolution from a variety of micron sized powders of Pd; the Pd·Ni·Zr oxide nano-compounds supplied by BA and other samples containing Pd examined so far in our laboratory [14–17]. Special emphasis is laid on the time-resolved characteristics as well as effect of oxidation of the samples on the sorption characteristics.

2. Experimental Apparatus

The twin absorption system for hydrogen isotope absorption experiments is composed of two identical parts, A_1 and A_2, one of which is as shown in Fig. 1. Palladium nano-particles are put in the reaction chamber, and the outer chamber is evacuated for thermal insulation during hydrogen isotope sorption. The reservoir tank is filled with D_2 (H_2) gas at a pressure of 0.4 MPa, typically, before an absorption run starts. The flow rate of D_2 (or H_2) gas is adjusted and regulated with a "Super Needle" valve.

Note: This paper is prepared for the Proceeding of *ICCF16*, Chennai, India, 2011.

†E-mail: kitamuraakira3@gmail.com
‡Also at: Technova Inc., Uchisaiwaicho 1-1-1, Chiyodaku, Tokyo 100-0011, Japan.
§Also at: Osaka University, Suita 5650871, Japan.

Table 1. Sample characteristics.

Sample name	Supplier	Composition (molar ratio)			Averaged particle size (nm)	Specific surface area (m^2/g)	Weight of Pd· Ni (g) in the sample
		Pd	Ni	Zr			
PP	Nilaco	1	–	–		100	10
PB	Nilaco	1	–	–			10
PZ	Santoku Corp.	0.321	–	0.679	41.3	8.3	2.78
PNZ2B	B. Ahern	0.04	0.29	0.67	0.5	2–5	0.39+1.56

Sheath heaters with resistance of 110.0 Ω in A_1 and 36.1 Ω in A_2 are used for sample baking, and also for sample heating in the cases of forced deoxidation and forced oxidation. Alumel–chromel thermo-couples are used to measure temperatures.

For calorimetry, the coolant water is maintained constant (±0.1˚C) at near-room temperature with a chiller, and the flow rate is controlled with a digital coolant transmitter at a rate of 6 cm^3/min, which recovers heat with an efficiency of 82.5±8.1%. There is a delay in the response of the temperature difference due to the indicial response with a time constant (τ) of 5.2 min. Calorific power is calculated from temperature difference between the exit and the entrance of the water-coolant. The calibrated conversion factor is 0.51 W/K.

The samples used in the present work include the 0.1-μm-diam. Pd powder "PP" (Nilaco Corporation), 300-mesh Pd-black powder "PB" (Nilaco Corp.), a Pd·Zr oxide composite "PZ" (Santoku Corporation), a Ni·Zr oxide composite "NZ" (Santoku Corp.), a Pd·Ni·Zr oxide composite "PNZ" (Santoku Corp.), and another Pd·Ni·Zr oxide composite "PNZ2B" provided by BA with the melt-spinning method. Composition and particle size of these samples are compared in Table 1. One of the most important parameters is the particle fineness or "fractality".

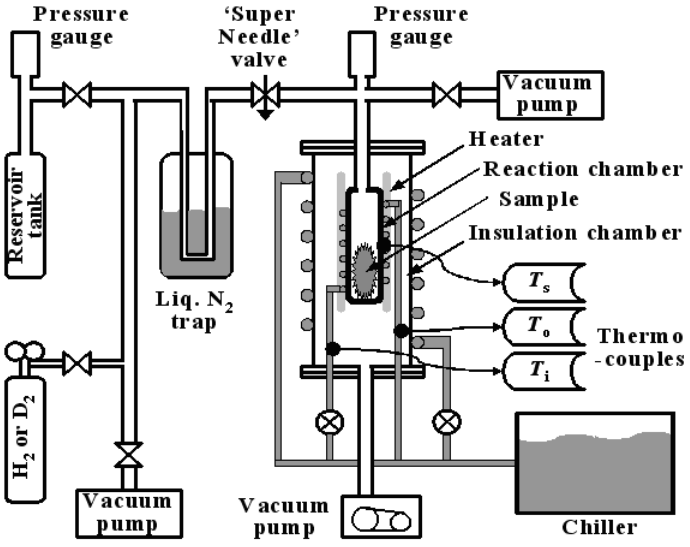

Figure 1. Schematic of one part of the twin system.

3. Experimental Procedure and Data Processing

Figure 2 shows the experimental procedure. The as-received sample containing PdO (and NiO) is baked at 440 K for 2 h in vacuum, and subjected to the D_2 (H_2) absorption run (No. 1 run). The sample is reused either without any treatment (A or B run) or after the specified treatment; forced deoxidation (No. 2 run) or forced oxidation (No. 3 run). In the case of the forced deoxidation, the sample is heated after filling the reaction chamber with the hydrogen isotope gas at a pressure of 0.3 MPa, and kept at 570 K for 24 h. On the other hand, in the case of the forced oxidation, the sample is treated in the similar manner using oxygen gas at a pressure of 0.4 MPa kept at 470 K or 570 K for 30 h. The fraction x of the oxidized atoms, [PdO·NiO]/[Pd·Ni], is calculated from the pressure drop during this procedure.

In Nos. 1 and 3 runs for the sample containing oxygen, the released heat might include energy of oxygen pickup reaction, Q_{red}[eV/atom-O], and that of hydrogen isotope absorption/adsorption, the 'hydridation' energy, $Q_{D(H)}$[eV/atom-D(H)];

$$\mathrm{Pd(Ni)O}_x + \left(x + \frac{y}{2}\right)\mathrm{D}_2 = x\mathrm{D_2O} + \mathrm{Pd(Ni)D}_y + xQ_{\mathrm{red}} + yQ_{\mathrm{D}}, \tag{1}$$

$$\mathrm{Pd(Ni)O}_x + \left(x + \tfrac{y}{2}\right)\mathrm{H}_2 = x\mathrm{H_2O} + \mathrm{Pd(Ni)H}_y + xQ_{\mathrm{red}} + yQ_{\mathrm{H}}, \tag{2}$$

where x is the fraction of Pd (Ni) atoms oxidized, and y is the fraction of Pd (Ni) atoms hydrogenated. We have assumed here that all of the $\mathrm{Pd(Ni)O}_x$ atoms are deoxidized under exposure of hydrogen based on an observation that the Nos. 3A and 3B runs gave almost the same absorption parameters as those for No. 2 run.

The total chemical energy released might include the energy of adsorption onto the surface of the ZrO_2 supporter as a result of a possible spill-over effect. Since it is difficult to distinguish experimentally the contribution of the spilled-over hydrogen atoms from y, we assume here that both y and $Q_{\mathrm{D(H)}}$could include the contributions not only

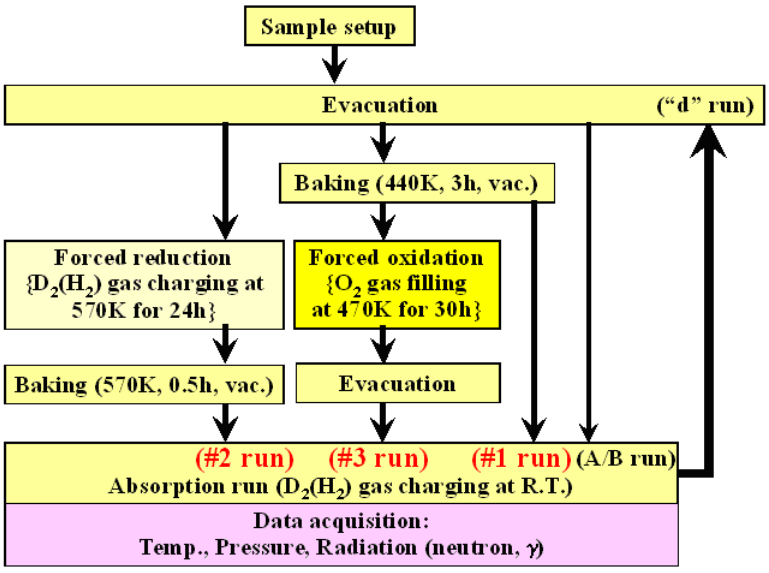

Figure 2. Flowchart of the experimental procedure.

from the absorption into the Pd/Pd·Ni bulk lattice but also adsorption onto the surfaces of the Pd/Pd·Ni nano-particle and the supporter. Thus the total chemical output energy, which is observed as the first-phase output energy E_1, as will be seen in the following paragraphs, is expressed as

$$E_1 = x\,Q_{\mathrm{red}} + y\,Q_{\mathrm{D(H)}}. \tag{3}$$

The energies of formation of oxides associated in the present phenomena for the bulk samples not under influence of nano-structure are as follows:

$$\mathrm{Pd} + \tfrac{1}{2}\mathrm{O_2} \rightarrow \mathrm{PdO} + Q_{\mathrm{PdO}} (Q_{\mathrm{PdO}} = 0.886\ \mathrm{eV}), \tag{4}$$

$$\mathrm{Ni} + \tfrac{1}{2}\mathrm{O_2} \rightarrow \mathrm{NiO} + Q_{\mathrm{NiO}} (Q_{\mathrm{NiO}} = 2.478\ \mathrm{eV}), \tag{5}$$

$$\mathrm{D_2} + \tfrac{1}{2}\mathrm{O_2} \rightarrow \mathrm{D_2O} + Q_{\mathrm{D_2O}} (Q_{\mathrm{D_2O}} = 2.654\ \mathrm{eV}), \tag{6}$$

$$\mathrm{H_2} + \frac{1}{2}\mathrm{O_2} \rightarrow \mathrm{H_2O} + Q_{\mathrm{H_2O}} (Q_{\mathrm{H_2O}} = 2.511\ \mathrm{eV}). \tag{7}$$

The energies of the oxygen pickup reactions, Q_{red}, are calculated by combining the above equations;

$$\mathrm{PdO} + \mathrm{D_2} \rightarrow \mathrm{Pd} + \mathrm{D_2O} + Q_{\mathrm{red}}^{\mathrm{Pd,D}}, \qquad Q_{\mathrm{red}}^{\mathrm{Pd,D}} = Q_{\mathrm{D_2O}} - Q_{\mathrm{PdO}} = 1.768\ \mathrm{eV}, \tag{8}$$

$$\mathrm{PdO} + \mathrm{H_2} \rightarrow \mathrm{Pd} + \mathrm{H_2O} + Q_{\mathrm{red}}^{\mathrm{Pd,H}}, \qquad Q_{\mathrm{red}}^{\mathrm{Pd,H}} = Q_{\mathrm{H_2O}} - Q_{\mathrm{PdO}} = 1.6\ 25\mathrm{eV}, \tag{9}$$

$$\mathrm{NiO} + \mathrm{D_2} \rightarrow \mathrm{Ni} + \mathrm{D_2O} + Q_{\mathrm{red}}^{\mathrm{Ni,D}}, \qquad Q_{\mathrm{red}}^{\mathrm{Ni,D}} = Q_{\mathrm{D_2O}} - Q_{\mathrm{NiO}} = 0.176\ \mathrm{eV}, \tag{10}$$

$$\mathrm{NiO} + \mathrm{H_2} \rightarrow \mathrm{Ni} + \mathrm{H_2O} + Q_{\mathrm{red}}^{\mathrm{Ni,H}}, \qquad Q_{\mathrm{red}}^{\mathrm{Ni,H}} = Q_{\mathrm{H_2O}} - Q_{\mathrm{NiO}} = 0.033\ \mathrm{eV}. \tag{11}$$

We note that the energies of the oxygen pickup reactions for PdO, in Eqs. (**??**) and (**??**), are of the order of magnitude larger than those for NiO, in Eqs. (**??**) and (**??**).

We have to use Eq. (**??**) to know the value of $yQ_{\mathrm{D(H)}}$ by subtracting the first term xQ_{red} from the value of E_1 obtained experimentally. However, in the case of No. 1 run we do not know x, the fractions of PdO and NiO, independently from y. We want to determine $(x + y/2)$ in Eqs. (**??**) and (**??**) from decrease in the number of gas-phase atoms, ΔN, calculated by changes in the pressure of the reservoir and the reaction chambers. If the water, D_2O or H_2O, remains in the gas phase with the same volume as D_2/H_2, then the decrease ΔN is due solely to $y/2$, the absorption/adsorption. On the other hand, if the water atoms condensate into the liquid phase or adsorbed not only on the sample surfaces but also on the inner surface of the reaction chamber and pipes, the water formation is also responsible to the decrease ΔN. We have no means to experimentally determine the fraction of x to be subtracted from the decrease ΔN to determine y.

In the case of No. 3 run, we know x. However, we have found a problem: if we assume that all the oxygen atoms which would give a pressure in excess of the vapor pressure of 4 kPa at room temperature are condensed, we have

too small, sometimes negative, values of $yQ_{D(H)}$. In the present work, we therefore calculate $yQ_{D(H)}$ by assuming that $xQ_{red} = 0$ first, and evaluate the error when the proper values of x and the cited values of Q_{red} for bulky samples are assumed. The assumption that $Q_{red}$is negligible, or equivalently that the values of the oxidation energy Q_{PdO} and Q_{NiO} are very much enhanced for the nano-particle samples, could be reasonable, just by the same reason as the assumption that the hydridation energy $Q_{D(H)}$ is enhanced significantly for the nano-particle samples, which, as will be seen later, we want to make one of the most important conclusion of the present work.

Another important parameter is the differential heat of hydrogen uptake [3], which is calculated in the present work as the time-resolved sorption energy per one hydrogen atom absorbed/adsorbed [18,20]

$$\eta\,(t) \approx \frac{\int_t^{t+\Delta t} \overline{W(t,\tau)}\,\mathrm{d}t}{L(t+\Delta t)-L(t)}, \tag{12}$$

where $L(t)$ is the time-resolved loading ratio, and

$$\overline{W\,(t,\,\tau)} = \frac{\int_t^{t+\tau} W_{\mathrm{meas}}\,(t)\;\mathrm{d}t}{\tau} \tag{13}$$

is the measured output power per one Pd atom, $W_{meas}(t)$, averaged over the time constant τ of the calorimetry system. The averaging was necessary, since the measured power has an indicial response of exponential delay with the time constant of $\tau = 5.2$ min. The numerator of Eq. (**??**) is the output energy per one Pd atom during a time interval of Δt, and the denominator is the number of the hydrogen atom absorbed/adsorbed per one Pd atom during the same interval. The value of $\eta(t)$ is averaged over the time interval of Δt, which is arbitrarily chosen here to be the time constant of the calorimetry;$\Delta t = \tau$. The averaging was necessary, since the scattering in the data of $L(t)$ was rather large.

4. Results and Discussion

4.1. Characteristics of the PZ sample

It was shown in Refs. [16,17] that the absorption characteristics of the Pd particles are strongly dependent on the particle size. Here the results are briefly summarized. The PZ sample showed much larger loading ratio, D/Pd and H/Pd, and the first-phase specific absorption/adsorption energy, E_1, than those for the PP sample and the PB sample. Figure 3 shows (a) typical variation of the heat evolution, W_D and W_H, pressure in the reaction chamber, P_D and P_H, the loading ratio, L_D and L_H, and the time-resolved specific sorption energy, η_D, and η_H, and (b) the $L(t)$–$P(t)$ diagram in the hydrogen isotope absorption runs after forced oxidation, D-PZ13# 3 and H-PZ14# 3, for the PZ samples containing 2.78 g of Pd. The first phase is defined as the duration of the run during which absorption of hydrogen (deuterium/protium) is terminated, or the loading ratio L_D/L_H reaches a steady-state value. In the second phase, there were observed sometimes anomalous temperature hump possibly suggesting an anomalous heat evolution in the deuterium absorption runs [16], however with poor reproducibility. In the following, we pay attention only to the first-phase parameters in the present paper.

The first-phase-integrated parameters for the samples PZ#1 through PZ#14 are shown as histograms in Fig. 4. To evaluate $Q_{D(H)}$ in No. 3 runs with use of Eq. (**??**), as has been explained above, we have ignored the contribution of the oxygen pickup reaction to the output energy, i.e., $xQ_{red} = 0$. This is because $yQ_{D(H)}$ was calculated to be negative, if we used the cited values of Q_{red}, Eqs. (**??**) and (**??**), for bulky samples. Later in this paper we will find other bases to assume that xQ_{red} should be negligible for the nano-particle samples.

The first-phase was found to be divided into two sub-phases, the 1a-phase and the 1b-phase [18]. In the 1a-phase, rapid absorption/adsorption occurred with high heat output, $\eta_{1a} \sim 1.0$ eV/atom-D(H), probably in the near-surface

region.Treatment of the sample by oxygen or oxygen incorporation into the sample was necessary for this phase to appear.The η_{1aD} value was larger than η_{1aH}usually by up to 20%, but by several times in some periods of time. However, no isotope effect was observed in the $L(t)$–$P(t)$ diagram in the 1a-phase [18].

The 1b-phase had a lower heat output nearly equal to the published value for the bulky Pd sample, $\eta_{1b} \sim 0.2$–0.3 eV/atom-D(H) with little isotopic difference. On the other hand, a significant isotope effect was observed in the $L(t)$–$P(t)$ diagram. The H_2 pressure in the 1b-phase was $P_{1bH} \sim 2$–6 kPa, while the D_2 pressure was about $P_{1bD} \sim 10$ kPa [18]. The isotope effect is of the same nature as that observed by Laesser and Klatt [1]. The difference could be accounted for by a difference in the velocity-dependent probability of tunneling penetration through the periodic potential well in the bulk lattice.

A possible interpretation of the absence of the 1a-phase in No. 2 run might be simply that the baking condition was not sufficient to purge the adsorbed hydrogen out of the surface adsorption sites that could have become deeper due to a nano-size effect. On the other hand, it could also be possible to assume an active role of oxygen in Nos. 1 and 3 runs to make strong absorption sites with significantly attracting dangling bonds to enhance the 1a-phase sorption parameters. The consequence might be a concentration of hydrogen atoms to form the 4D-TSC [20].

4.2. Similar effect of oxidation observed in the PP and PB sample runs

The distinguished effect of oxidation has been examined also for the PP and the PB samples. Figure 5(a) shows typical variation of $W_{D(H)}$, $P_{D(H)}$, $L_{D(H)}$ and $\eta_{D(H)}$ in the hydrogen-isotope absorption runs for the PP samples containing 10 g of Pd after forced oxidation (O/Pd $\sim$ 0.019), D-PP3#3 and H-PP4#3, whose $L(t)$–$P(t)$ diagrams are shown in Fig. 5(b).

We notice the presence of the 1a-phase and the 1b-phase similarly to the PZ sample. The 1a-phase, appearing only in Nos. 1 and 3 runs containing oxygen, has a saturation pressure of $P_{1a} \sim 10$ kPa, which is about twice as high as that

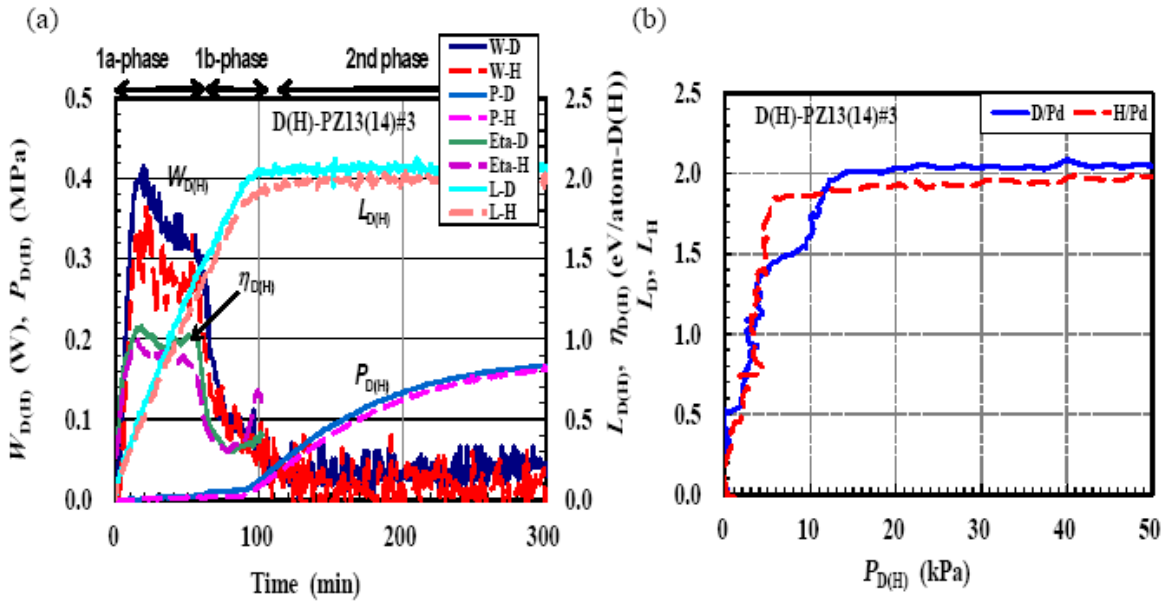

Figure 3. (a) Typical traces of output power $W(t)$, pressure $P(t)$, time-resolved loading ratio $L(t)$ and time-resolved specific sorption energy $\eta(t)$, (b) $L(t) - P(t)$ diagram of the PZ13(14)# 3 runs.

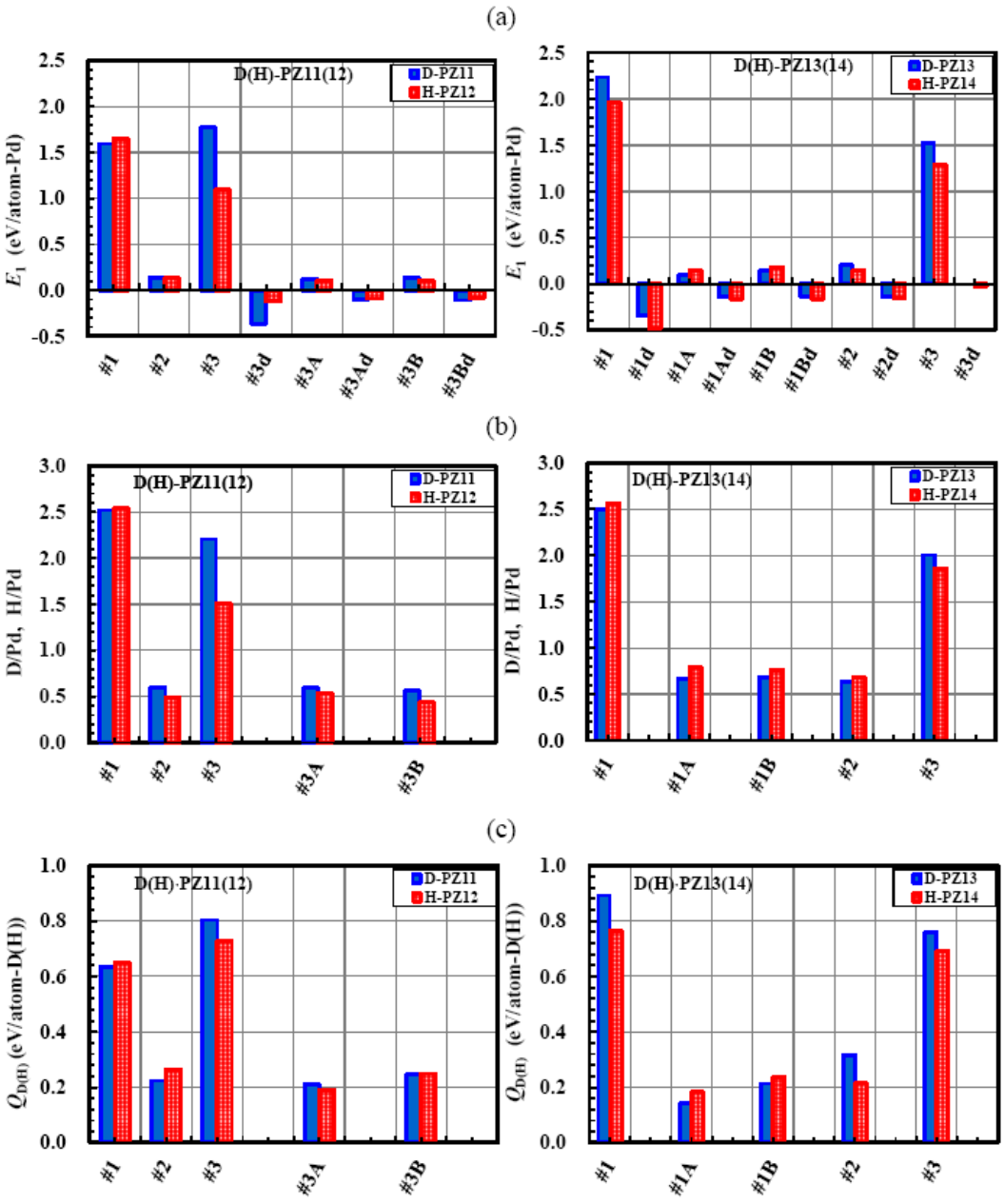

Figure 4. First-phase absorption parameters of the PZ sample; (a) first-phase specific output energy, E_1, (b) the loading ratio, D(H)/Pd, and (c) the hydridation energy, $Q_{D(H)}$.

in the case of the PZ sample, and even higher than the saturated water vapor pressure of 4 kPa at room temperature. The 1a-phase is followed by the 1b-phase with a plateau pressure of $P_{1bD} \sim 12$ kPa and $P_{1bH} \sim 18$ kPa in the D and H run, respectively. Water, if any, appears to have been in unsaturated or supersaturated vapor state. If condensation of water vapor occurred, there should have been a significant pressure hump, as will be seen in the PNZ2B runs.

The first-phase parameters for the PP sample are summarized in Fig. 6. The PP#1, PP#2 and PP#3A runs have almost the same values of the first-phase specific output energy E_1, the loading ratio D(H)/Pd and the hydridation energy $Q_{D(H)}$ as those for the PZ#1A, PZ#1B, PZ#2, PZ#3A and PZ#3B runs, which are considered to be characteristic of the bulk Pd sample with no oxygen.

The PP samples have the oxidation effect similar, but modest, to that for the PZ samples. The PP#3 runs after forced oxidation have about 50% larger values of E_1 and $Q_{D(H)}$. What is important is that the difference cannot be explained only by a contribution of the oxygen pickup reaction, xQ_{red}, which is indicated by the arrow in Fig. 6(c), if any. We recognize that the effect of oxygen incorporation is not only through the simple oxygen pickup reaction but also by some active function to deepen the potential well for the hydrogen isotopes.

The PB samples also showed absorption characteristics similar to the PP and the PZ samples. Typical traces of E_1, $P(t)$, $L(t)$ and $\eta(t)$ of the D-PB5#3 and the H-PZ6#3 runs are shown in Fig. 7(a), with the $L(t)$–$P(t)$ diagram in Fig. 7(b), and the first-phase absorption parameters in Fig. 8. We see the absorption parameters have the medium values compared to the PP and the PZ samples. The effect of oxygen treatment/incorporation is universal for the Pd nano-particles, and becomes more significant as the particle fineness increases; i.e., in the order of the PP-sample, the PB-sample and the PZ-sample.

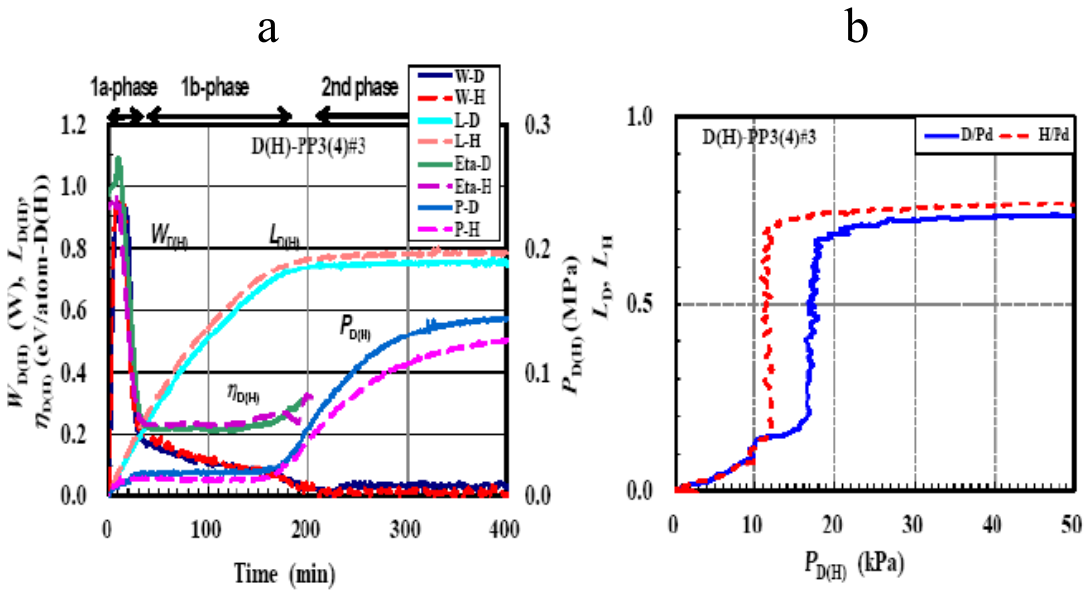

Figure 5. (a) Output power $W(t)$, pressure $P(t)$, time-resolved loading ratio $L(t)$ and time-resolved specific sorption energy $\eta(t)$, (b) $L(t) - P(t)$ diagram of the PP3(4) #3 runs.

4.3. Peculiar effects observed in the PNZ2B sample runs

The PNZ2B sample contains Pd·Ni binary nano-particles dispersed in ZrO_2 matrix [19] with an atomic ratio of about Pd_4Ni_{29}. Typical traces of the absorption parameters are shown in Fig. 9-(1a), (2a) and (3a) for the Nos. 1–3 runs of the 10-g aliquots of D-PNZ2B4 and the H-PNZ2B3 samples each containing 0.39 g of Pd and 1.56 g of Ni. Here we notice that the PNZ2B samples have significantly large values of the output power as well as of the loading ratio. Since we know that pure Ni samples absorb very little amount of hydrogen isotopes at room temperature, the large values

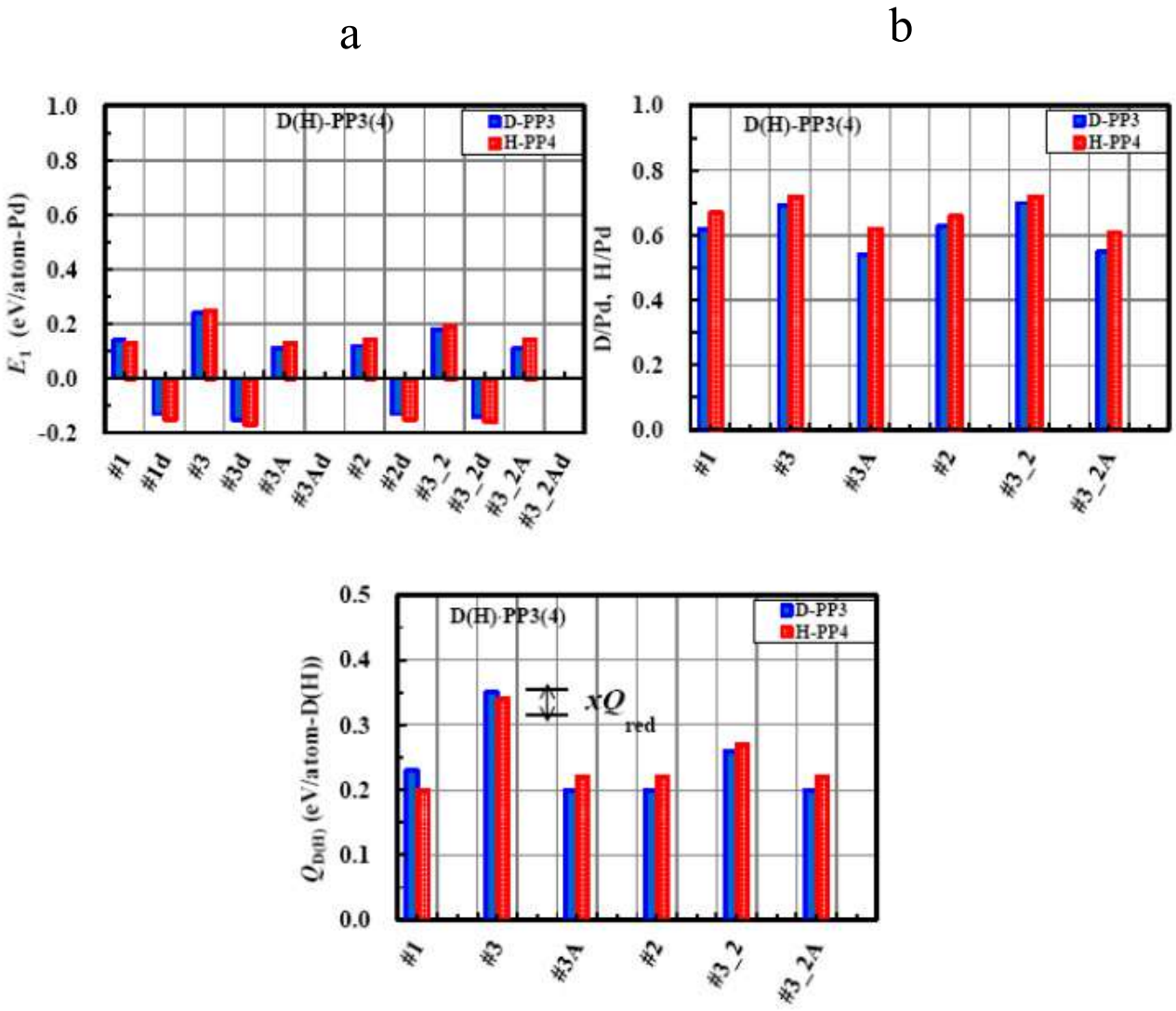

Figure 6. First-phase parameters of the D-PP3#3 and the H-PP4#3 runs.

of the absorption parameters are ascribed to the existence of a small amount of Pd added to Ni and/or to the dispersed structure itself of the PNZ2B sample prepared by the melt-spinning method.

The PNZ2B samples showed peculiar pressure changes. Figure 9-(1b), (2b) and (3b) shows the $L(t)$–$P(t)$ diagram for the D-PNZ2B4 and H-PNZ2B3runs. One of the distinctive features is that Nos. 1 and 3 runs have pressure humps in the early stage of the first phase. The gas sorption became significant after the pressure increased to several tens of kPa.

This behavior, never observed in the runs usingthe samples other than PNZ2B, could be ascribed to possible existence of NiO layers covering the surface of the Pd·Ni nano-particles. The surface NiO layer is relatively hard to be deoxidized. However, once the deoxidation reaction (**??**) or (**??**) with a small reaction energy occurs at a point on the surface and a pit with a dangling bond on the surface of the Pd·Ni nano-particle is exposed to ambient D_2 / H_2 atmosphere, rapid dissociation to D/H atoms could be initiated at the pit, and rushing of the hydrogen atoms into the bulk would follow, which results in the rapid decrease in the pressure. This could be possible, since the hydrogen adsorption and absorption of Ni are as easy as those of Pd having almost the same values of adsorption and absorption energies [21]. However, we know that the samples had very little amount of oxygen atoms after each absorption run. Complete deoxidation during No. 1 run and No. 3 run should therefore be concluded. So the above story seems to be not probable.

Another interpretation of the pressure behavior could be condensation of supersaturated water vapor produced from the hydrogen and oxygen in/on the sample contained in the as-received (No. 1) and the oxidized (No. 3) samples. If this is the case, the assumption could be justified that there occurred no water condensation in the PP, PB and PZ runs, which had no humps in the pressure traces.

Figure 10 shows the absorption parameters E_1, D(H)/[Pd·Ni] and $Q_{D(H)}$ as histograms. In evaluating $Q_{D(H)}$ using Eq. (**??**), no contribution of the term xQ_{red} has also been assumed here. The most remarkable feature of the PNZ2B

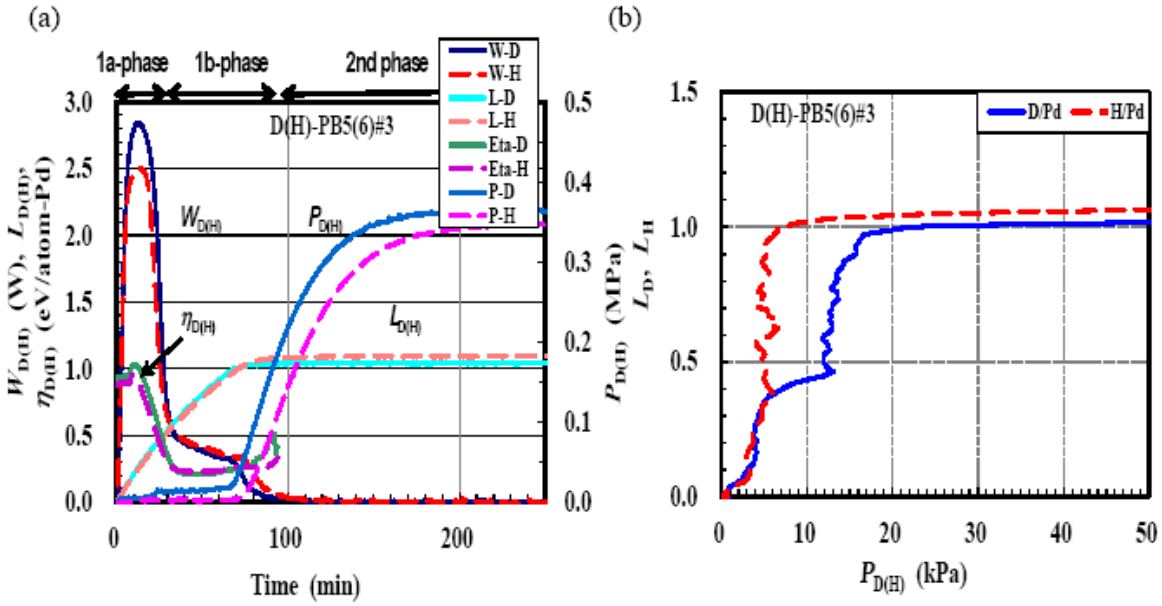

Figure 7. (a) Output power $W(t)$, pressure $P(t)$, time-resolved loading ratio $L(t)$ and time-resolved specific sorption energy $\eta(t)$, (b) $L(t) - P(t)$ diagram of the PB5(6)#3 runs.

sample is that No. 2 runs have almost the same values of the absorption parameters as those for the No. 1 and the No. 3 runs. This is exactly the reason why we neglected xQ_{red} in evaluating $yQ_{\mathrm{D(H)}}$. Otherwise, we have values of $yQ_{\mathrm{D(H)}}$=0.6–0.7 eV/atom-Pd·Ni, the first term in Eq. (**??**). This is a contradiction, since the value is much smaller than the values of $E_1 = yQ_{\mathrm{D(H)}}$ = 1.0–1.8 eV/atom-Pd·Ni in No. 2 runs having no contribution of xQ_{red}. We have to exclude the possibility that substantial amount of xQ_{red} should be subtracted from E_1 in Nos. 3 and 1 runs, or in other words, we have to conclude that $Q_{\mathrm{red}} \approx 0$ for our nano-particle samples, as is discussed later in this section.

We also neglected x in evaluating y from a similar reason. If we subtract x = 1.4–1.7 indicated by the oxidation fraction in No. 3 runs, then we have D(H)/[Pd·Ni] = 1.4–1.5 which is much smaller than those in No. 2 runs. Since the pressure humps in the $P(t)$ traces and $L(t)$–$P(t)$ diagrams are thought to be due to condensation of water vapor, we certainly have nonzero contribution from water.

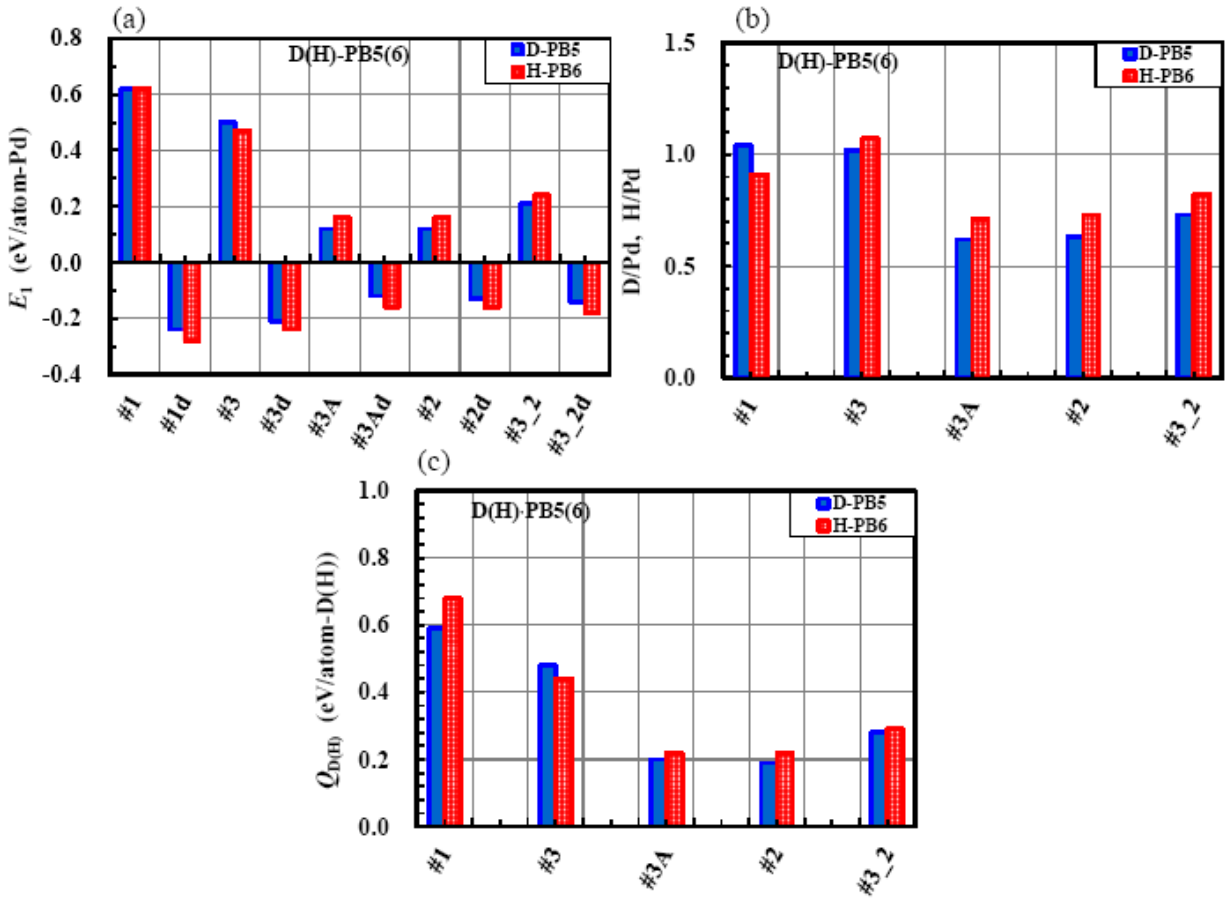

Figure 8. First-phase parameters of the D-PB5#3 and the H-PB6#3 runs.

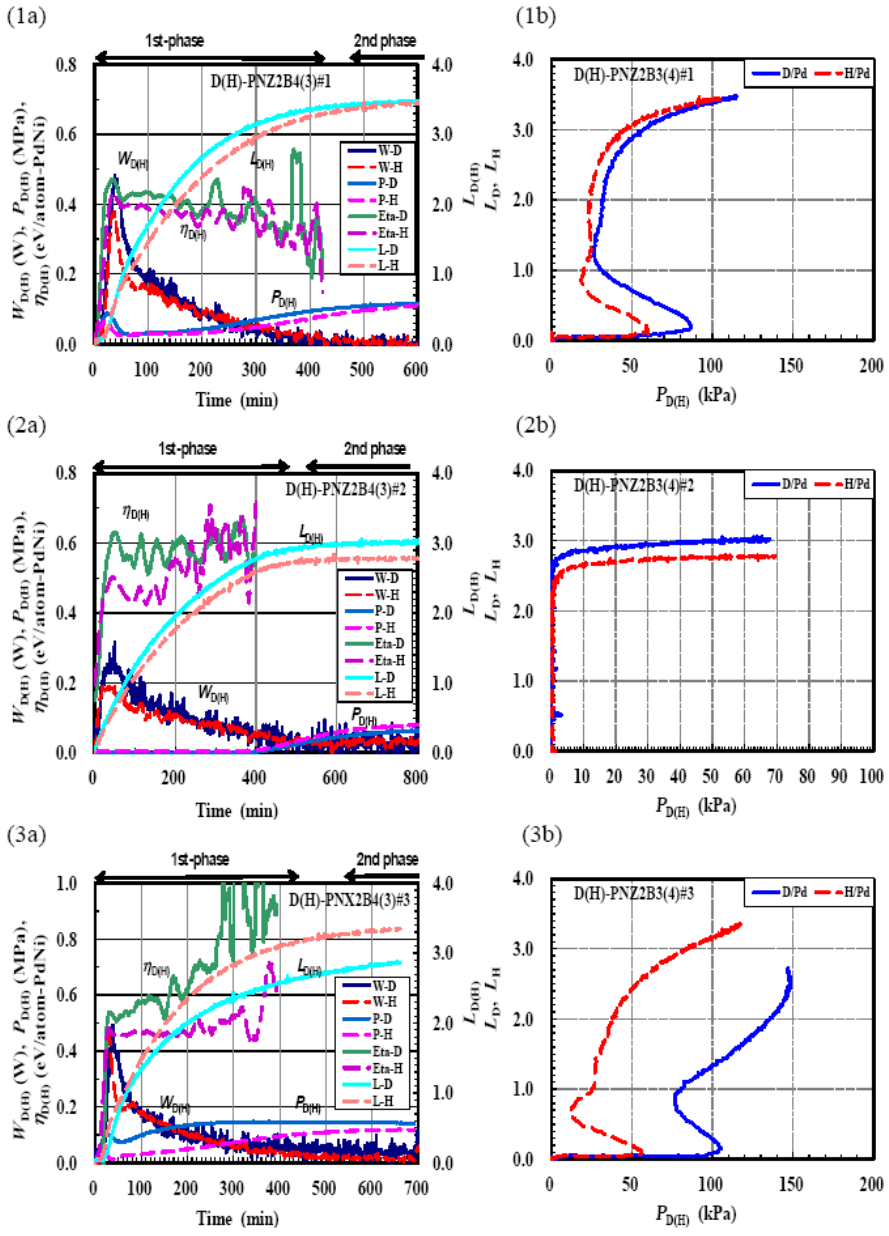

Figure 9. (1a,2a,3a) Output power $W(t)$, pressure $P(t)$, time-resolved loading ratio $L(t)$ and time-resolved specific sorption energy $\eta(t)$, (1b,2b,3b) $L(t)$–$P(t)$ diagram of the H(D)-PNZ2B3(**??**)#1, H(D)-PNZ2B3(**??**)#2 and H(D)-PNZ2B3(**??**)#3 runs.

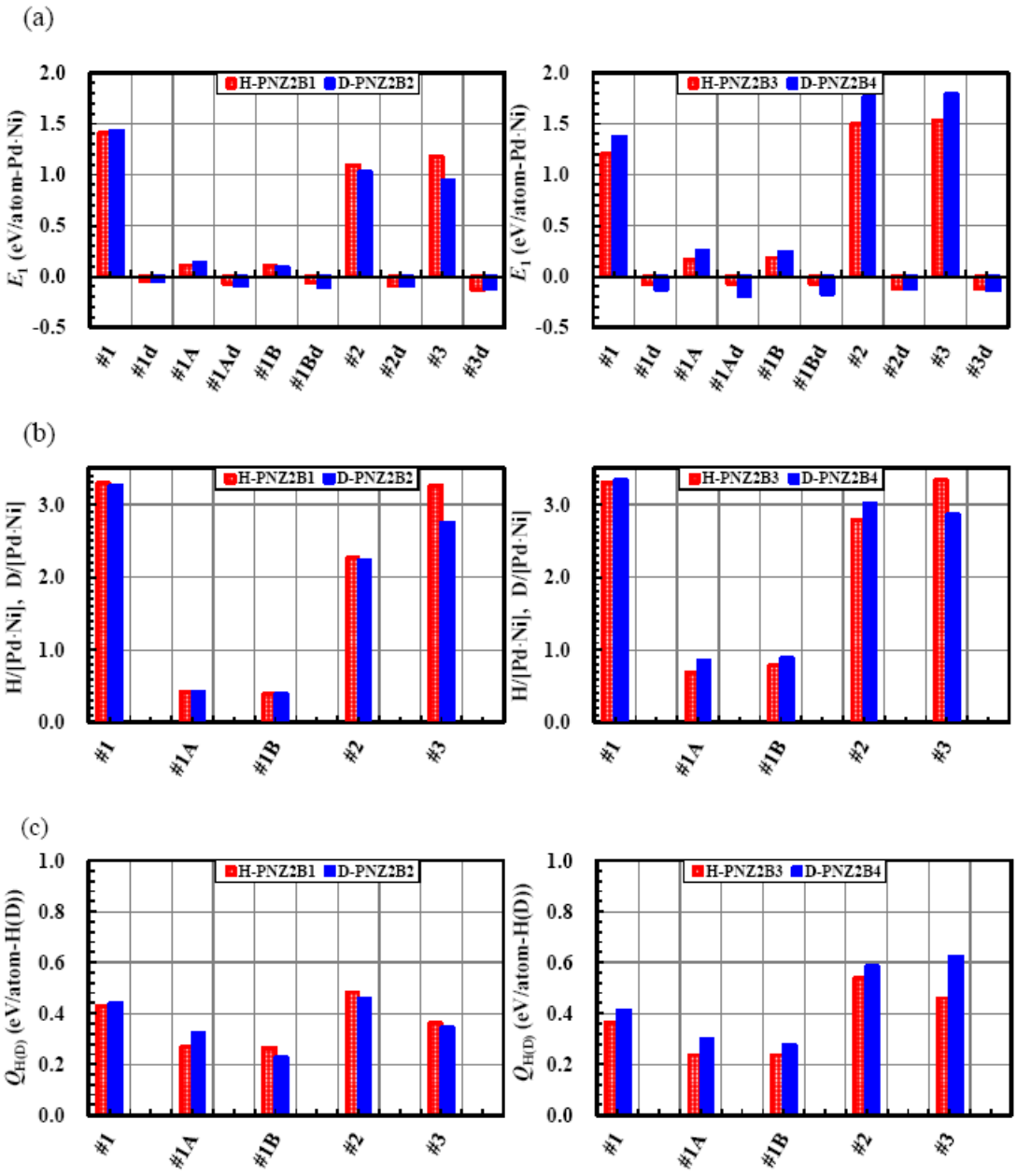

Figure 10. First-phase absorption parameters of the samples PNZ2B1 through PNZ2B4.

We have to have an additional diagnostic tool to measure x independently, e.g., a residual gas mass analyzer.

The finally saturated value of the loading ratio, D(H)/[Pd·Ni], is extraordinarily large; 2.1 or larger not only in Nos. 1 and 3 runs but also in No. 2 run for the sample containing no oxygen. The large values of the loading ratio could be explained by adsorption on the supporter (ZrO_2) surface and/or in the grain boundaries via the so-called spill-over effect catalyzed by small amount of Pd atoms on the Ni nano-particle surface. An assumption that hydrogen isotopes are loaded both into the tetrahedral and octahedral sites seems to be too bold.

The No. 2 samples absorb/adsorb almost the same amount of hydrogen with almost the same sorption energy as those in Nos. 1 and 3 runs. This fact can be explained by an assumption that the baking condition of 0.5 h at 570 K was sufficient to purge almost all the hydrogen atoms adsorbed and absorbed in the preceding runs and the forced deoxidation process. This is consistent with the relatively small values of $Q_{\mathrm{D(H)}} \approx 0.4$ eV/atom-D(H) shown in Fig. 10 (c) compared with those for the PP, the PB and the PZ samples.

From this fact, we can be confident about the assumption of neglecting the term xQ_{red} in evaluating $yQ_{\mathrm{D(H)}}$ using Eq. (**??**). Since x is not negligible at least for the PNZ2B sample, we may conclude that the oxygen pickup energy Q_{red}in Eqs. (**??**)–(**??**) is reduced to small values as a result of a nano-size effect. This is equivalent to a deduction that oxidation energies, Q_{PdO} and Q_{NiO}, are significantly increased for the nano-particle samples due to the nano-size effect.

Another distinctive feature is that the pressure in the first-phase of No. 2 run is too low to notice the isotope effect in the $L(t)$–$P(t)$ diagram. This could be due to an unknown effect of the nano-particle-dispersed structure, or to that of the Ni nano-particle itself. At the moment, we have no further information to determine what the case is.

Next, we notice that $\eta_{\mathrm{D(H)}}$ is relatively constant throughout a run with the mean value lying between 0.4 and 0.6 eV/atom-D(H), in accordance with the absence of the sub-phase transition. This is in contrast to the PZ, PP and PB samples whose first-phases were divided into the 1a- and the 1b-phases. The mean values for the PNZ2B samples are rather modest compared with those (∼1 eV/atom-D(H))in the 1a-phase of other sample runs.This is a consequence of large $L_{\mathrm{D(H)}}(t)$ for the PNZ2B sample.

Finally it should be pointed out that in all cases of Nos. 1–3 runs, the averaged value of $\eta_D$for deuterium is larger than that of $\eta_H$for protium, sometimes by a factor of 1.5 or more. This might indicate that some nuclear effects including nuclear reactions could contribute to the heat evolution.

5. Summary

Deuterium and protium gas absorption/adsorption by a variety of Pd nano-powders has been examined using a twin absorption system. The powders include ∼0.1-μmϕPd powder (PP), Pd-black (PB), Pd nano-particles (∼10 nmϕ) admixed with ZrO_2 (PZ) and Pd·Ni binary nano-particles (∼2 nmϕ) dispersed in ZrO_2 holder-flakes (PNZ2B). The first-phase parameters of the absorption runs for the PP, the PB and the PZ samples are summarized as follows:

(1) Both the deoxidized samples and those reused without baking process showed essentially the same values of 0.62 ± 0.04 (0.70 ± 0.06) for the loading ratio D(H)/Pd, and 0.14 ± 0.03 (0.16 ± 0.01) eV/atom-Pd for the specific output energy $E_{1D(H)}$. The resultant hydridation energy $Q_{\mathrm{D(H)}}$ = 0.23 ± 0.05 (0.23 ± 0.01) eV/atom-D(H) is consistent with the published value of the inter-lattice absorption energy for bulky samples.

(2) For the as-received and oxidized samples the values of D(H)/Pd and E_1 are both increasing functions of fineness of the Pd surface, and exceeds 2.0 and 1.5 eV/atom-Pd, respectively, for the PZ sample. The hydridation energy $Q_{\mathrm{D(H)}}$ = 0.83 ± 0.06 (0.72 ± 0.05) eV/atom-D(H) is substantially larger than the published value of 0.5 eV/atom-D(H) for the surface adsorption energy.

(3) Time-resolved measurements of pressure and heat output revealed sub-phase (1a to 1b) transition in the first-phase for the as-received and the oxidized samples. The 1a-phase, characterized by rapid absorption/adsorption and high heat output, is found to be characteristic of nano-particles containing oxygen, probably caused by the

process occurring in the near-surface region. A rather large isotope effect in the differential heat of sorption, $\eta_{D(H)}$, has sometimes been observed in the 1a-phase. The 1b-phase, on the other hand, is thought to be due to absorption into the bulk with significant isotope effect on the loading-pressure relation, $L(t)$–$P(t)$.

The $Pd_{0.04}Ni_{0.29}Zr_{0.67}$ oxide composite sample, PNZ2B, has unique properties summarized as follows:

(1) The observed loading ratio, D(H)/[Pd·Ni] $\approx 3.2 \pm 0.3$ (3.4 ± 0.1), and the specific heat release, $E_1 \approx 1.4 \pm 0.3$ (1.2 ± 0.3) eV/atom-[Pd·Ni], in the first-phase of the as-received and the oxidized sample runs are both very large, while the hydridation energy $Q_{D(H)}$ = 0.45 ± 0.12 (0.33 ± 0.09) eV/atom-D(H) is nearly equal to the mean value of the surface hydrogen adsorption energy and the absorption energy of bulky Pd. It is inferred that the Pd atoms act as a catalyst for the hydrogen isotope absorption/adsorption of Ni at room temperature.
(2) An important difference between the PNZ2B sample and other Pd samples is that the No. 2 run after the forced deoxidation has essentially the same values of the absorption parameters as those of Nos. 1 and 3 runs. It is inferred that the surface adsorption potential is shall-ower for the PNZ2B sample than for the Pd-based samples.
(3) The as-received and the oxidized PNZ2B samples show anomalous change of gas pressure in the beginning of the first-phase, which is thought to be due to condensation of water.
(4) The time-dependent sorption energy is rather constant at$\eta_{D(H)} \approx$ 0.60 (0.53) eV/atom-D(H) with no 1a–1b sub-phase transition. The ratio η_D/η_H is sometimes greater than 1.5, which appears to be suggesting the existence of heat component of nuclear origin.

References

[1] R. Laesser and K.-H. Klatt; Solubility of hydrogen isotopes in palladium, *Phys. Rev. B* **28** (1983) 748–758.
[2] M.A. Chou and P. Vannice; Calorimetric heat of adsorption measurements of palladium: 1. Influence of crystallite size and support on hydrogen adsorption, *J. Catalysis* **104** (1987) 1–16.
[3] S.-Y. Huang, C.-D. Huang, B.-T. Chang and C.-T. Yeh; Chemical activity of palladium clusters: sorption of hydrogen; *J. Phys. Chem. B* **110** (2006) 21783–21787.
[4] For example, E. Storms, Status of cold fusion; *Naturwiss* .**97** (2010) 861–881.
[5] Y. Arata and Y. Zhang; The special report on research project for creation of new energy; *J. High Temperature Society* **34** (2008) 85–93.
[6] Y. Arata and Y. Zhang; Development of "DS-Reactor" as the practical reactor of "Cold Fusion" based on the "DS-Cell" with "DS-Cathode"; In Takahashi A (Ed.) Condensed Matter Nuclear Science, *Proc. 12th Int. Conf. on Cold Fusion*, World Scientific, Singapore, 2006, pp. 44–54.
[7] V.A. Kirkinskii and A.I. Khmelnikov; Setup or measuring of energy balance at interaction of metals and hydrogen isotopes gas at high temperatures and pressures, *Proc. ICCF13*, Sochi, 2007, Publisher Center MATI, Moscow (ISBN 978-5-93271-428-7) pp. 43–46.
[8] J.P. Biberian and N. Armanet, Excess heat production during D_2diffusion through palladium, *Proc. ICCF13*, Sochi, 2007. Publisher Center MATI, Moscow (ISBN 978-5-93271-428-7) pp. 170–180.
[9] F. Celani, P. Marini, V. di Stefano, M. Nakamura, O.M. Calamai, A. Spallone, E. Purchi, V. Andreassi, B. Ortenzi, E. Righi, G. Trenta, G. Cappuccio, D. Hampai, F. Piastra and A. Nuvoli; Towards a high temperature CMNS reactor: nano-coated Pd wires with D_2 at high pressures; http://iccf15.frascati.enea.it/ICCF15-PRESENTATIONS/S4_O3_Celani.pdf.
[10] D. Kidwell, A. Rogers, K. Grabowski and D. Knies, Does gas loading produce anomalous heat?;http://iccf15.frascati.enea.it/ICCF15-PRESENTATIONS/S4_O6_Kidwell.pdf. (2009).
[11] T. Hioki, H. Azuma, T. Nishi, A. Itoh, J. Gao, S. Hibi, T. Motohiro and J. Kasagi, Hydrogen/deuterium absorption property of Pd fine particle systems and heat evolution associated with hydrogen/deuterium loading, *Proc. ICCF-15*, 2009, Rome, Italy, 2011.
[12] T. Hioki, H. Azuma, T. Nishi, A. Itoh, S. Hibi, J. Gao, T. Motohiro and J. Kasagi; Absorption capacity and heat evolution

with loading of hydrogen isotope gases for Pd nanopowder and Pd/ceramics nanocomposite, *J. Condensed Matter Nucl. Sci.* **4** (2011) 69–80.

[13] O. Dmitriyeva, R. Cantwell, M. McConnell, G. Moddel, Deuterium and hydrogen loading into nano-Pd on zeolite and alumina matrices at low pressures, 9^{th} *Int. Work shop on Anomalies in Hydrogen/Deuterium Loaded Metals*, 2010, Sienna, Italy.

[14] T. Nohmi, Y. Sasaki, T. Yamaguchi, A. Taniike, A. Kitamura, A. Takahashi, R. Seto and Y. Fujita, Basic research on condensed matter nuclear reaction using Pd powders charged with high density deuterium; http://www.ler-canr.org; *Proc. 14th Int. Conf. Condensed Matter Nucl. Sci. (ICCF14)*, Washington, DC, 2008.

[15] Y. Sasaki, A. Kitamura, Y. Miyoshi, T. Nohmi, A. Taniike, A. Takahashi, R. Seto and Y. Fujita; Anomalous heat generation in charging of Pd powders with high density hydrogen isotopes -(I). Results of absorption experiments using Pd powders; http://iccf15.frascati.enea.it/ICCF15-PRESENTATIONS/S7_O5_Sasaki.pdf.

[16] A. Kitamura, T. Nohmi, Y. Sasaki, A. Taniike, A. Takahashi, R. Seto and Y. Fujita; Anomalous effects in charging of Pd powders with high density hydrogen isotopes, *Phys. Lett. A* **373** (2009) 3109–3112.

[17] A. Kitamura, Y. Sasaki, Y. Miyoshi, A. Taniike, A. Takahashi, R. Seto and Y. Fujita, Heat Evolution from Pd nano-powders exposed to high-pressurehydrogen isotopes and associated radiation measurements, *J. Condensed Matter Nucl. Sci.* **4** (2011) 56–68.

[18] A. Kitamura, Y. Miyoshi, H. Sakoh, A. Taniike, A. Takahashi, R. Seto and Y. Fujita, Time-resolved measurements of loading ratios and heat evolution in D_2 (and H_2)–Pd·Zr mixed-oxide systems, *J. Condensed Matter Nucl. Sci.* **5** (2011) 42–51.

[19] B. Ahern, Private communication, 2011.

[20] A. Takahashi, A. Kitamura, Y. Sasaki, Y. Miyoshi, A. Taniike, A. Takahashi, R. Seto and Y. Fujita, Role of PdO surface-coating of Pd nano-particle for D(H) charging and cluster fusion, *Proc. 10th Meeting of Japan-CF Research Society*, 2010, pp. 46–53.

[21] Y. Fukai, K. Tanaka and H. Uchida, *Hydrogen and Metals* (Uchida Rokakuho, Tokyo, 1998) [in Japanese].